Deep-Ultraviolet Frequency Metrology of H2 for Tests of Molecular Quantum Theory

Altmann, R. K.; Dreissen, L. S.; Salumbides, E. J.; Ubachs, W.; Eikema, K. S.E.

published in
Physical Review Letters
2018

DOI (link to publisher)
10.1103/PhysRevLett.120.043204

document version
Publisher's PDF, also known as Version of record

Deep-Ultraviolet Frequency Metrology of H_2 for Tests of Molecular Quantum Theory

R. K. Altmann, L. S. Dreissen, E. J. Salumbides, W. Ubachs, and K. S. E. Eikema
LaserLaB, Department of Physics and Astronomy, VU University Amsterdam, De Boelelaan 1081, 1081 HV Amsterdam, Netherlands

(Received 23 July 2017; published 25 January 2018)

Molecular hydrogen and its isotopic and ionic species are benchmark systems for testing quantum chemical theory. Advances in molecular energy structure calculations enable the experimental verification of quantum electrodynamics and potentially a determination of the proton charge radius from H_2 spectroscopy. We measure the ground state energy in ortho-H_2 relative to the first electronically excited state by Ramsey-comb laser spectroscopy on the $EF\,^1\Sigma_g^+$-$X\,^1\Sigma_g^+(0,0)$ $Q1$ transition. The resulting transition frequency of 2 971 234 992 965(73) kHz is 2 orders of magnitude more accurate than previous measurements. This paves the way for a considerably improved determination of the dissociation energy (D_0) for fundamental tests with molecular hydrogen.

DOI: 10.1103/PhysRevLett.120.043204

The fully quantized version of electrodynamics (QED) constitutes an important part of the standard model and is arguably the best tested theory in physics, based (among other experiments) on spectroscopic measurements of atomic hydrogen [1–3]. The molecular counterpart, H_2, has served as the model system for molecular quantum theory dating back to 1927, when Heitler and London first explained the existence of a bound state between two hydrogen atoms [4]. Although the increased complexity of the electronic structure and the additional vibrational and rotational degrees of freedom impose serious theoretical and experimental challenges, it also provides additional opportunities to explore new physics. Measurements of various level energies [5–10] are in excellent agreement with the most recent theoretical predictions [11–13]. Comparisons between the experimental results and theory provide constraints on possible physics beyond the standard model, such as hypothetical fifth forces and extra dimensions [14–17]. In particular, the dissociation energy of molecular hydrogen $D_0(H_2)$ serves as an important benchmark number for molecular quantum physics, and it has stimulated improvements by 7 orders of magnitude in its experimental and theoretical determinations over nearly a century [18].

On the theoretical side, a number of refined calculations have been performed to verify and improve the initial results [19]. The Born-Oppenheimer potential of H_2 was calculated to 10^{-15} precision [20], the adiabatic correction was improved by 3 orders of magnitude to 3×10^{-7} cm^{-1} [12], nonadiabatic corrections of rovibrational levels were calculated to 10^{-7} cm^{-1} precision [13], the $m\alpha^6$ QED corrections were explicitly calculated [21], and methods to solve the Schrödinger equation were improved [22]. This heroic program led to a value of $D_0(H_2) = 36\,118.0691\,(6)$ cm^{-1}, which is more accurate but consistent with the initial value [19]. Moreover, recent breakthroughs in calculating the molecular structure and QED now indicate that it will become feasible to determine the proton-charge radius from a sufficiently accurate determination of $D_0(H_2)$ [21,22]. This is particularly interesting in view of the proton-charge radius puzzle [23–27].

To obtain an experimental value of D_0, it can be related to the ionization energy $E_I(H_2)$ via a thermodynamic cycle involving the well-known atomic ionization energy $E_I(H)$ and dissociation energy of the ion $D_0(H_2^+)$ [5]. The value $E_I(H_2)$ can in turn be determined experimentally by measuring two frequency intervals ($EF - X$ and $54p1_1 - EF$) by laser spectroscopy and, as a third step, the extrapolation of the np-Rydberg series measured with millimeter wave excitation [28]. In Fig. 1, the energy intervals and their relations are shown to obtain a new value for $D_0(H_2)$ by measuring $E_I(H_2)$ (see also [18]).

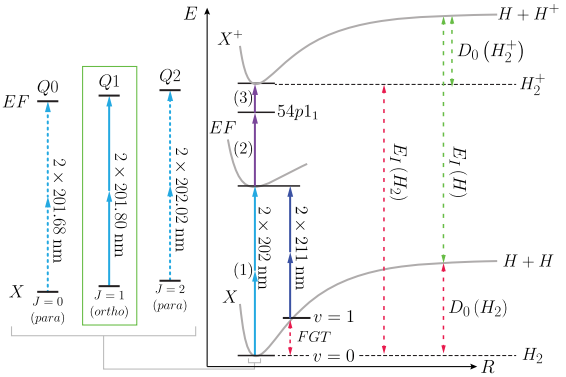

FIG. 1. Simplified energy level diagram of H_2. Interesting numbers in view of testing molecular QED are, e.g., the dissociation energy (D_0) and the fundamental ground tone (FGT). For this purpose, we measured the deep-ultraviolet two-photon $Q1$ line, as indicated on the left.

Previous experimental values for D_0 [5] were found to be in good agreement at a level of 0.0004 cm^{-1} (12 MHz) with molecular quantum calculations [19]. Agreement was also obtained for D_2 [6], and both results featured thereupon in interpretations in terms of constraints on fifth forces [16] and extra dimensions [15] for typical intramolecular distances at the 1 Å scale.

In this Letter, we report on a determination of the $EF^1\Sigma_g^+$-$X^1\Sigma_g^+(0,0)$ $Q1$ transition in H_2 [as discussed before, an essential ingredient for determining $D_0(H_2)$] with a nearly 2 orders of magnitude improved accuracy compared to previous measurements [29,30]. We employ Ramsey-comb two-photon spectroscopy [31,32] in the ultraviolet at 201.80 nm, achieving a fractional uncertainty of 2.5×10^{-11}.

Our experimental approach of Ramsey-comb spectroscopy [31,32] combines Ramsey's method of separated oscillatory fields [33] with frequency-comb lasers [34,35]. It utilizes the interference between two excitation contributions in an atom or molecule induced by two time-delayed coherent laser pulses. This leads to a variation of the excited state population ($|c_e|^2$) as a function of the pulse delay (t) and pulse phase difference ($\Delta\phi$) according to

$$|c_e(t,\Delta\phi)|^2 \propto \cos(2\pi f_{\mathrm{tr}} t + \Delta\phi). \quad (1)$$

The transition frequency (f_{tr}) can be determined from this signal, provided that t and $\Delta\phi$ are known with sufficient precision [36,37]. Frequency-comb lasers are therefore a convenient source of light pulses, as their repetitive pulsed output (with spacing T_{rep}) and controlled phase difference between successive pulses (the carrier-envelope phase slip $\Delta\phi_{\mathrm{ceo}}$) can be referenced with high accuracy to an atomic clock.

To increase the pulse energy of frequency combs for nonlinear frequency up-conversion, amplification and enhancement resonators have been employed to reach the microjoule level pulse energy at a full repetition rate [38–41]. In contrast, our method relies on the amplification of only two pulses, enabling an orders of magnitude higher pulse energy (> mJ). By choosing pulse pairs with a delay of multiples of T_{rep} and scanning the pulse delay on a much smaller scale using adjustments of T_{rep} via the comb laser, a series of Ramsey signals starting at time delays $t = T_0 = \Delta N T_{\mathrm{rep}}$ is obtained. Here ΔN is an integer, denoting the delay expressed in the number of comb laser pulses. Combining a series of Ramsey signals for different ΔN constitutes a Ramsey-comb measurement [32]. The transition frequency is obtained from it by analyzing only the relative phase evolution between the Ramsey signals [42]. As a consequence, the measurement becomes insensitive to any phase shift that is independent of ΔN. This includes a possible constant phase shift caused by the amplification and nonlinear up-conversion of the frequency-comb pulses and also phase shifts induced in the atom by the laser-atom interaction (the ac-Stark shift), provided that the pulse energy is constant as a function of ΔN. The accuracy of the method is mainly limited by the maximum time delay that one can experimentally achieve and the accuracy of how constant $\Delta\phi$ is as a function of ΔN.

The starting point of the experimental setup is a Kerr-lens mode-locked Ti:sapphire frequency-comb laser, operating at a repetition time of $T_{\mathrm{rep}} = 7.9$ ns ($f_{\mathrm{rep}} = 1/T_{\mathrm{rep}} =$ 126 MHz). Both T_{rep} and $\Delta\phi_{\mathrm{ceo}}$ are actively stabilized and referenced to a cesium atomic clock (Symmetricon CsIII 4310B) to provide an absolute time and frequency calibration. The comb laser pulses are chirped by 2.5×10^6 fs^2 of second-order dispersion in a $4f$-grating based stretcher for chirped-pulse amplification. In addition, an adjustable slit placed in the Fourier plane of the stretcher selects only 0.2–0.3 nm bandwidth of the frequency-comb spectrum centered around 807.18 nm, resulting in pulses of approximately 10–15 ps duration and an energy of 40 pJ. The small bandwidth is chosen to only excite the $Q1$ line in H_2 and avoid excitation of the nearby $Q0$ and $Q2$ lines, which are at, respectively, 806.73 and 808.09 nm in terms of the fundamental frequency-comb wavelength (see Fig. 1). Only two comb pulses are selectively amplified (at a repetition rate of 28 Hz) in a noncollinear optical parametric chirped-pulse amplifier to a pulse energy of 2.4 mJ (for details, see [43–45]). The amplified pulses are up-converted to the fourth harmonic by frequency doubling and two stages of sum-frequency mixing to produce 62 μJ of 201.80 radiation; see Fig. 2.

The two-photon transition is excited with counterpropagating pulses to suppress the first-order Doppler shift. In both arms, a quarter wave plate is used to convert linear to circular polarization. Together with the strong chirp on the

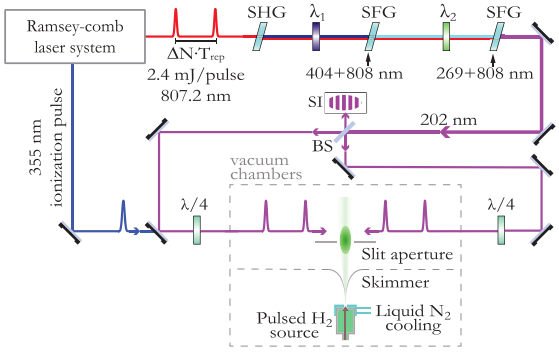

FIG. 2. Schematic overview of the experimental setup. Amplified comb pulse pairs are frequency up-converted in sequential doubling (SHG) and mixing (SFG) stages in β-barium borate. Between each stage, a special wave plate (λ_1 and λ_2) rotates the polarization to maintain type-I phase matching. The generated 201.80 nm beam is split equally by a metallic beam splitter (BS) where they recombine again after one round-trip to form a Sagnac interferometer (SI). The molecular beam is formed from a pulsed supersonic expansion and is collimated by a skimmer and subsequent slit aperture.

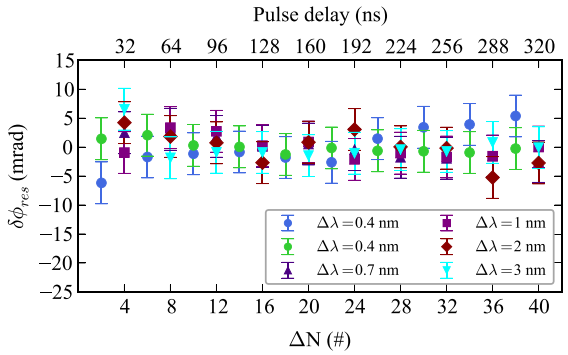

FIG. 3. Measurements of the relative phase shift between the first and second excitation pulse in the infrared as a function of the delay time between the pulses. Measurements for various bandwidths from 3 down to 0.4 nm (two sets) were performed (indicated by the different markers and colors). No systematic effects as a function of the bandwidth are observed.

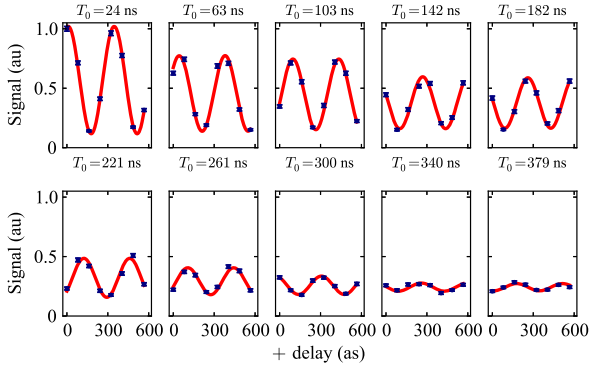

FIG. 4. Example of a Ramsey-comb measurement with a step size of $\Delta N = 5$, where each Ramsey scan starts at $T_0 = \Delta N T_{\mathrm{rep}}$. The signal is shown as blue data points, and the fit (red line) is based on Eq. (1).

pulses [46,47], this suppresses unwanted (Doppler shifted) excitation from a single side by a factor of 10. The intersection point of the ultraviolet pulses is crossed at right angles with a collimated beam of hydrogen molecules from a pulsed supersonic expansion. A laser pulse at 355 nm provides state-selective ionization, and the created H_2^+ ions are extracted through a 25 cm time-of-flight drift tube and detected with an electron multiplier (ETP AF880) and Stanford Research SR250 boxcar integrator.

The well-defined phase relation of the original frequency-comb pulses can be distorted by the amplification process, and any delay-time-dependent component ($\delta\phi_{\mathrm{res}}$) will lead to a frequency shift proportional to $\delta\phi_{\mathrm{res}}/\Delta N T_{\mathrm{rep}}$ [44]. We verify the phase of the amplified pulses using spectral interferometry with the unamplified comb laser pulses [31,32]. The optimum bandwidth of the laser pulses (0.2–0.3 nm) for H_2 excitation reduces the number of spectral fringes in the phase measurement, hampering its accuracy. Therefore, we measured the phase effects for bandwidths ranging from 3 down to 0.4 nm, as shown in Fig. 3. The calculated frequency shifts for these measurements are between −26 and 42 kHz, all with an uncertainty of 40 kHz, and do not show any significant trend. Therefore, we take the value of 14(40) kHz at $\Delta\lambda =$ 0.4 nm to be representative, as it is closest to the 0.2–0.3 nm bandwidth used for the excitation.

In Fig. 4, an example of a Ramsey-comb measurement is shown where the pulse delay is varied up to a maximum time delay of 380 ns ($\Delta N = 48$ pulses). The reduction of the signal and modulation contrast as a function of delay is caused by effects such as the laser linewidth, Doppler broadening, transit time, and the lifetime of the excited state (≈200 ns) [48]. A typical Ramsey-comb measurement consists of sets of three or four Ramsey scans over a maximum time delay between 181 and 221 ns, which is chosen for optimal signal to noise and speed of measurement to minimize the influence of drifts. The minimum delay used is $\Delta N = 2$ to avoid potential transient effects. At each ΔN, the repetition time is scanned over a range of 600 as to observe ∼1.5 periods of the Ramsey signal. A statistical uncertainty of 45 kHz for a single Ramsey-comb measurement was expected based on the fluctuations of the ion signal (monitored over 500 laser shots), but in practice it was 1.9 times larger. As no correlation could be found with any experimental parameter, we increased the statistical error with a Birge factor [49,50] of 1.9.

Concerning systematic effects, the first- and second-order Doppler shifts have to be carefully considered, as the hydrogen molecules have a speed of 2530 m/s due to the supersonic expansion at 311 K. The excitation geometry strongly suppresses the first-order Doppler shift, but a residual first-order Doppler shift can still be present due to an asymmetry in the spectrum, a chirp-induced first-order Doppler shift [3], or a residual angle between the two counterpropagating beams. As a first step to minimize these effects, the counterpropagating beams are aligned as parallel as possible by observing a dark fringe at the output port of the Sagnac interferometer (see Fig. 2). Any residual Doppler effect after this procedure (on the order of ±200 kHz) is detected by changing the velocity of the

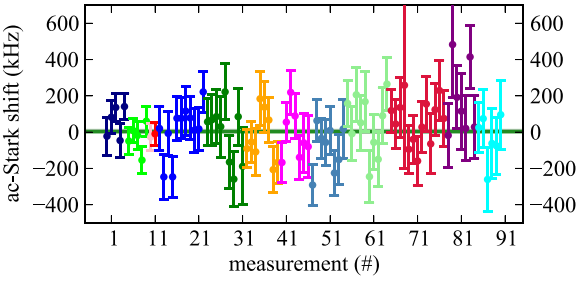

FIG. 5. Light shift measurements (see the text). Each point is the ac-Stark shift at 62 μJ per pulse, based on an extrapolation to zero energy from measurements performed at 18 and 62 μJ per pulse. The different colors indicate measurements taken on different days, and each data point consist of at least four Ramsey-comb measurements.

TABLE I. Contributions (in kilohertz) to the measurement of the $Q1$ transition in H_2. The light-induced effects include the ac-Stark shift and nonlinear effects.

	Measured value	(1σ)
Doppler-free transition frequency	2 971 234 992 948	(60)
Light-induced effects	3	(13)
dc-Stark shift	0	(2)
Zeeman shift	0	(2)
Amplifier phase-induced shift	14	(40)
Total	2 971 234 992 965	(73)

molecular beam. To this end, the nozzle is cooled to 97 K by liquid nitrogen, leading to a most probable velocity of 1420 m/s. The Doppler-free transition frequency can then be determined by extrapolating the measured transition frequencies at both temperatures to zero velocity (taking a $\pm 10\%$ velocity uncertainty into account). In this procedure, the second-order Doppler shift correction of 107 and 33 kHz for 2530 and 1420 m/s was taken into account. In total, seven sets of measurements were obtained to determine the Doppler-free transition frequency, each consisting of 20 or more Ramsey-comb measurements at both temperatures (and therefore velocity). All measurements are in agreement with each other within the statistical uncertainty, leading to a weighted average of all measurements (before other corrections) of 2 971 234 992 948(60) kHz.

Although the Ramsey-comb method is to first order insensitive to effects proportional to the pulse energy (such as the ac-Stark effect or phase shifts in the up-conversion), a residual light shift might still be present. We test this by measuring the transition frequency at pulse energies of 18 and 62 μJ (the energy at which all other measurements were performed, within 5%). Extrapolation to zero intensity then gives the shift at 62 μJ pulse energy. In total, 91 determinations of this kind are taken into account, each consisting of at least four Ramsey-comb measurements (Fig. 5). The resulting light shift correction is 3(13) kHz, showing that the Ramsey-comb method is for all practical purposes ac-Stark shift free.

A dc-Stark shift is avoided by ramping up the ion-extraction fields after the ionization pulse. The remaining field uncertainty of ± 0.17 V/cm leads to a shift of 0(2) kHz. Magnetic fields (leading to the Zeeman effect) were minimized by external compensation coils to 0.2 G, so that no shift is expected within 2 kHz.

It should be considered that for ortho-hydrogen the total nuclear spin $I = 1$, which leads to hyperfine structure in the $Q1$ line. The splitting in the ground state is too small ($\lesssim$500 kHz) to be observed [51] and in the excited state unknown. Therefore, the presented value is a weighted average of the hyperfine components of the $Q1$ line. The $Q0$ transition from the true ground state in para-hydrogen does not have hyperfine structure but is 3 times weaker due to spin statistics. For this reason, $Q1$ was measured in the current and previous experiments.

Taking all effects into account results in a transition frequency of 2 971 234 992 965(73) kHz for the $EF^1\Sigma_g^+$-$X^1\Sigma_g^+(0,0)$ $Q1$ transition in ortho-H_2 (see Table I). The relative uncertainty of this result is 2.5×10^{-11} and is in agreement with the previous measurement [29] but 2 orders of magnitude more accurate (see Table II). The new two-photon transition frequency of the $Q1$ line of ortho-hydrogen can be used to obtain an improved value for the (rotationless) dissociation energy $D_0(H_2)$ of para-hydrogen, using the procedure from Ref. [5]. The result is consistent with previous experimental determinations and the theory, as shown in Table II.

However, in a recent study a complete calculation of the relativistic corrections was targeted to reach a full-fledged molecular quantum calculation [52]. In Ref. [19], the relativistic correction was partially based on an older study [53]. The new refined calculation surprisingly produces a disagreement of 50 MHz (0.0017 cm^{-1}) with the previous and current experimental values, equal to 2.4σ (see Table II). However, as the authors state, this disagreement is to be considered preliminary, since relativistic nuclear recoil corrections have not yet been reliably calculated. Our result now shows that possible deviations are not due to measurements of the $EF - X$ interval, given its new highly accurate value.

The full potential of our measurement can be reached only if the energy separation between $X^+ - EF$ is improved to a level comparable with 70 kHz or better, to bring down the uncertainty of D_0 (H_2). This will enable us to put further constraints on the strength of fifth forces [14] and on the compactification sizes of extra dimensions

TABLE II. Contributions to the determination of D_0 in H_2 in cm^{-1} and the comparison with the latest theoretical values.

Transition	Previous results	This result	Theory	Deviation
(1) $EF \leftarrow X$	99 109.731 39(18) [29]	99 109.731 204 9(24)		0.000 19(18)
(2) $54p1_1 \leftarrow EF$	25 209.997 56(29) [5]			
(3) $X^+ \leftarrow 54p1_1$	42.270 539(10) [28]			
D_0	36 188.069 62(37) [5]	36 118.069 45(31)	36 118.069 5(10) [19]	0.000 1(10)
			36 118.069 1(6) [21]	−0.000 4(7)
			36 118.067 8(6) [52]	−0.001 7(7)

[15]. Moreover, given the ≈200 ns lifetime of the excited state, it seems feasible to ultimately reach 10 kHz accuracy on the $Q0$ transition (instead of $Q1$ to eliminate the influence of hyperfine structure). A theoretical and experimental comparison at this level would enable a determination of the proton-charge radius with an accuracy of 1%, therewith resolving the proton-charge radius puzzle. Furthermore, another benchmark test of the molecular quantum theory, the determination of the fundamental ground tone splitting (see Fig. 1), can be considerably improved now with a measurement of the $EF^1\Sigma_g^+$-$X^1\Sigma_g^+(0,1)$ $Q0$ transition.

[1] A. Matveev, C. G. Parthey, K. Predehl, J. Alnis, A. Beyer, R. Holzwarth, T. Udem, T. Wilken, N. Kolachevsky, M. Abgrall, D. Rovera, C. Salomon, P. Laurent, G. Grosche, O. Terra, T. Legero, H. Schnatz, S. Weyers, B. Altschul, and T. W. Hänsch, Phys. Rev. Lett. **110**, 230801 (2013).

[2] S. Galtier, H. Fleurbaey, S. Thomas, L. Julien, F. Biraben, and F. Nez, J. Phys. Chem. Ref. Data **44**, 031201 (2015).

[3] D. C. Yost, A. Matveev, A. Grinin, E. Peters, L. Maisenbacher, A. Beyer, R. Pohl, N. Kolachevsky, K. Khabarova, T. W. Hänsch, and T. Udem, Phys. Rev. A **93**, 042509 (2016).

[4] W. Heitler and F. London, Z. Phys. **44**, 455 (1927).

[5] J. Liu, E. J. Salumbides, U. Hollenstein, J. C. J. Koelemeij, K. S. E. Eikema, W. Ubachs, and F. Merkt, J. Chem. Phys. **130**, 174306 (2009).

[6] J. Liu, D. Sprecher, C. Jungen, W. Ubachs, and F. Merkt, J. Chem. Phys. **132**, 154301 (2010).

[7] E. J. Salumbides, G. D. Dickenson, T. I. Ivanov, and W. Ubachs, Phys. Rev. Lett. **107**, 043005 (2011).

[8] G. D. Dickenson, M. L. Niu, E. J. Salumbides, J. Komasa, K. S. E. Eikema, K. Pachucki, and W. Ubachs, Phys. Rev. Lett. **110**, 193601 (2013).

[9] M. L. Niu, E. J. Salumbides, and W. Ubachs, J. Chem. Phys. **143**, 081102 (2015).

[10] T. M. Trivikram, M. L. Niu, P. Wcislo, W. Ubachs, and E. J. Salumbides, Appl. Phys. B **122**, 294 (2016).

[11] J. Komasa, K. Piszczatowski, G. Łach, M. Przybytek, B. Jeziorski, and K. Pachucki, J. Chem. Theory Comput. **7**, 3105 (2011).

[12] K. Pachucki and J. Komasa, J. Chem. Phys. **141**, 224103 (2014).

[13] K. Pachucki and J. Komasa, J. Chem. Phys. **143**, 034111 (2015).

[14] E. J. Salumbides, J. C. J. Koelemeij, J. Komasa, K. Pachucki, K. S. E. Eikema, and W. Ubachs, Phys. Rev. D **87**, 112008 (2013).

[15] E. J. Salumbides, A. N. Schellekens, B. Gato-Rivera, and W. Ubachs, New J. Phys. **17**, 033015 (2015).

[16] W. Ubachs, J. C. J. Koelemeij, K. S. E. Eikema, and E. J. Salumbides, J. Mol. Spectrosc. **320**, 1 (2016).

[17] J. Biesheuvel, J. P. Karr, L. Hilico, K. S. E. Eikema, W. Ubachs, and J. C. J. Koelemeij, Nat. Commun. **7**, 10385 (2016).

[18] D. Sprecher, C. Jungen, W. Ubachs, and F. Merkt, Faraday Discuss. **150**, 51 (2011).

[19] K. Piszczatowski, G. Łach, M. Przybytek, J. Komasa, K. Pachucki, and B. Jeziorski, J. Chem. Theory Comput. **5**, 3039 (2009).

[20] K. Pachucki, Phys. Rev. A **82**, 032509 (2010).

[21] M. Puchalski, J. Komasa, P. Czachorowski, and K. Pachucki, Phys. Rev. Lett. **117**, 263002 (2016).

[22] K. Pachucki and J. Komasa, J. Chem. Phys. **144**, 164306 (2016).

[23] A. Antognini *et al.*, Science **339**, 417 (2013).

[24] R. Pohl, R. Gilman, G. A. Miller, and K. Pachucki, Annu. Rev. Nucl. Part. Sci. **63**, 175 (2013).

[25] R. Pohl *et al.*, CREMA Collaboration, Science **353**, 669 (2016).

[26] A. Antognini, K. Schuhmann, F. D. Amaro, P. Amaro, and F. Biraben, EPJ Web Conf. **113**, 01006 (2016).

[27] A. Beyer, L. Maisenbacher, A. Matveev, R. Pohl, K. Khabarova, A. Grinin, T. Lamour, D. C. Yost, T. W. Hänsch, and N. Kolachevsky, Science **358**, 79 (2017).

[28] A. Osterwalder, A. Wüest, F. Merkt, and C. Jungen, J. Chem. Phys. **121**, 11810 (2004).

[29] S. Hannemann, E. J. Salumbides, S. Witte, R. T. Zinkstok, E.-J. van Duijn, K. S. E. Eikema, and W. Ubachs, Phys. Rev. A **74**, 062514 (2006).

[30] A. Yiannopoulou, N. Melikechi, S. Gangopadhyay, J. C. Meiners, C. H. Cheng, and E. E. Eyler, Phys. Rev. A **73**, 022506 (2006).

[31] J. Morgenweg, I. Barmes, and K. S. E. Eikema, Nat. Phys. **10**, 30 (2014).

[32] R. K. Altmann, S. Galtier, L. S. Dreissen, and K. S. E. Eikema, Phys. Rev. Lett. **117**, 173201 (2016).

[33] N. F. Ramsey, Phys. Rev. **78**, 695 (1950).

[34] R. Holzwarth, T. Udem, T. W. Hansch, J. C. Knight, W. J. Wadsworth, and P. S. J. Russell, Phys. Rev. Lett. **85**, 2264 (2000).

[35] D. Jones, S. Diddams, J. Ranka, A. Stentz, R. Windeler, J. Hall, and S. Cundiff, Science **288**, 635 (2000).

[36] S. Witte, R. T. Zinkstok, W. Ubachs, W. Hogervorst, and K. S. E. Eikema, Science **307**, 400 (2005).

[37] D. Z. Kandula, C. Gohle, T. J. Pinkert, W. Ubachs, and K. S. E. Eikema, Phys. Rev. Lett. **105**, 063001 (2010).

[38] C. Gohle, T. Udem, M. Herrmann, J. Rauschenberger, R. Holzwarth, H. A. Schuessler, F. Krausz, and T. W. Hänsch, Nature (London) **436**, 234 (2005).

[39] A. Ozawa, W. Schneider, T. W. Hänsch, T. Udem, and P. Hommelhoff, New J. Phys. **11**, 083029 (2009).

[40] A. Cingoz, D. C. Yost, T. K. Allison, A. Ruehl, M. E. Fermann, I. Hartl, and J. Ye, Nature (London) **482**, 68 (2012).

[41] C. Benko, T. K. Allison, A. Cingöz, L. Hua, F. Labaye, D. C. Yost, and J. Ye, Nat. Photonics **8**, 530 (2014).

[42] J. Morgenweg and K. S. E. Eikema, Phys. Rev. A **89**, 052510 (2014).

[43] J. Morgenweg and K. S. E. Eikema, Opt. Lett. **37**, 208 (2012).

[44] J. Morgenweg and K. S. E. Eikema, Opt. Express **21**, 5275 (2013).

[45] S. Galtier, R. K. Altmann, L. S. Dreissen, and K. S. E. Eikema, Appl. Phys. B **123**, 16 (2017).

[46] A. Ozawa and Y. Kobayashi, Phys. Rev. A **86**, 022514 (2012).

[47] I. Barmes, S. Witte, and K. S. E. Eikema, Nat. Photonics **7**, 38 (2013).
[48] D. W. Chandler and L. R. Thorne, J. Chem. Phys. **85**, 1733 (1986).
[49] M. Henrion and B. Fischoff, Am. J. Phys. **54**, 791 (1986).
[50] G. Mana, E. Massa, and M. Predescu, Metrologia **49**, 492 (2012).
[51] N. F. Ramsey, Phys. Rev. **85**, 60 (1952).
[52] M. Puchalski, J. Komasa, and K. Pachucki, Phys. Rev. A **95**, 052506 (2017).
[53] L. Wolniewicz, J. Chem. Phys. **99**, 1851 (1993).